HHS Public Access

Author manuscript

Vis Neurosci. Author manuscript; available in PMC 2018 October 26.

Published in final edited form as:

Vis Neurosci. 2018 January ; 35: E004. doi:10.1017/S0952523817000359.

Melanopsin expression in the cornea

ANTON DELWIG[1,†], **SHAWNTA Y. CHANEY**[1], **ANDREA S. BERTKE**[2,‡], **JAN VERWEIJ**[1], **SUSANA QUIRCE**[6], **DELAINE D. LARSEN**[1], **CINDY YANG**[3,§], **ETHAN BUHR**[4], **RUSSELL VAN GELDER**[4], **JUANA GALLAR**[6], **TODD MARGOLIS**[1,2,**], and **DAVID R. COPENHAGEN**[1,5]

[1]Department of Ophthalmology, School of Medicine, University of California San Francisco, San Francisco, California

[2]Proctor Foundation, School of Medicine, University of California San Francisco, San Francisco, California

[3]Department of Anatomy, School of Medicine, University of California San Francisco, San Francisco, California

[4]Department of Ophthalmology, School of Medicine, University of Washington, Seattle, Washington

[5]Department of Physiology, School of Medicine, University of California San Francisco, San Francisco, California

[6]Instituto de Neurociencias de Alicante, Universidad Miguel Hernandez-CSIC, San Juan de Alicante, Spain

Abstract

A unique class of intrinsically photosensitive retinal ganglion cells in mammalian retinae has been recently discovered and characterized. These neurons can generate visual signals in the absence of inputs from rods and cones, the conventional photoreceptors in the visual system. These light sensitive ganglion cells (mRGCs) express the non-rod, non-cone photopigment melanopsin and play well documented roles in modulating pupil responses to light, photoentrainment of circadian rhythms, mood, sleep and other adaptive light functions. While most research efforts in mammals have focused on mRGCs in retina, recent studies reveal that melanopsin is expressed in non-retinal tissues. For example, light-evoked melanopsin activation in extra retinal tissue regulates pupil constriction in the iris and vasodilation in the vasculature of the heart and tail. As another example of nonretinal melanopsin expression we report here the previously unrecognized localization of this photopigment in nerve fibers within the cornea. Surprisingly, we were unable to detect light responses in the melanopsin-expressing corneal fibers in spite of our histological evidence based on genetically driven markers and antibody staining. We tested further for melanopsin localization

Address correspondence to: David R. Copenhagen, Departments of Ophthalmology and Physiology, School of Medicine, University of California San Francisco, 675 Nelson Rising Lane, San Francisco, CA 94158-0444. cope@phy.ucsf.edu.

†Present address: SiteOne Therapeutics, San Francisco, CA.

‡Present address: Department of Population Health Sciences, Virgini-Maryland College of Veterinary Medicine, Blacksburg, VA.

§Present address: Department of Neurobiology, UCLA.

**Present address: Department of Ophthalmology, Washington University School of Medicine, Saint Louis, MO.

Supplementary material

To view supplementary material for this article, please visit https://doi.org/10.1017/S0952523817000359.

in cell bodies of the trigeminal ganglia (TG), the principal nuclei of the peripheral nervous system that project sensory fibers to the cornea, and found expression of melanopsin mRNA ina subset of TG neurons. However, neither electrophysiological recordings nor calcium imaging revealed any light responsiveness in the melanopsin positive TG neurons. Given that we found no light-evoked activation of melanopsin-expressing fibers in cornea or in cell bodies in the TG, we propose that melanopsin protein might serve other sensory functions in the cornea. One justification for this idea is that melanopsin expressed in *Drosophila* photoreceptors can serve as a temperature sensor.

Keywords

Melanopsin; Trigeminal ganglion; Photosensitivity; Cornea

Introduction

The retina, a neural network located at the back of all vertebrate eyes, is the light sensitive tissue that supports vision. Light-sensing rod photoreceptors provide black and white vision and operate primarily in dim light. Cones serve to transduce light required for high acuity and color vision. A third class of photoreceptor in the retina comprised of the melanopsin-expressing ganglion cells (mRGCs) play important roles in adaptive and reflexive responses to light such as photoentrainment of circadian rhythms and pupillary constriction. Virtually, all research on melanopsin-expressing cells has centered on mRGCs in the retina. These studies have addressed phototransduction in the mRGCs, the morphology of distinct classes of mRGCs, the tracing of axonal projections to various brain areas, and the role of these cells in other adaptive or reflexive functions such as mood, sleep, and photophobia (Do & Yau, 2010; Lucas, 2013).

Melanopsin expression is found in cells outside of the retina. These extra-retinal localizations suggest that melanopsin-mediated functions are not necessarily directly associated with visual functions originating in mRGCs. The melanopsin expression has been observed in cells within the irides of mice, rats and other nonprimate mammals that are active at night or during twilight. In surgically isolated, *ex vivo* irides, these melanopsin cells mediate light-initiated pupil constriction (Xue et al., 2011). Additionally, the melanopsin expression has been reported in cell bodies of the trigeminal ganglia in mice. These authors also presented some evidence that a very small fraction of the TG neurons was stimulated by light (Matynia et al., 2016). Moreover, melanopsin is expressed in aortas and tail vessels of rats. Light activation of melanopsin evokes vasodilation in the tails and elicits relaxation of surgically isolated aortic rings (Sikka et al., 2014). Interestingly, a survey of G-protein coupled receptors in adult mice found significant accumulation of melanopsin mRNA in heart atria and ventricles (Regard et al., 2008). No visual function has been ascribed to melanopsin in these heart tissues.

Some evidence is emerging that melanopsin might be mediating nonvisual sensory functions. Locomotor tests show that *Drosophila* larvae can discriminate between different substrate temperatures. This temperature discrimination is lost in larvae in which the visual pigment rhodopsin is deleted genetically from photoreceptors. Unexpectedly, the genetically

engineered melanopsin expression in the photoreceptor cells lacking rhodopsin restores temperature discrimination (Shen et al., 2011). Therefore, in spite of intense focus on mRGCs in the retina, evidence is accumulating that melanopsin can be expressed outside of the retina and could be serving light-initiated or other sensory functions independently of mRGCs in the retina.

We tested the hypothesis that melanopsin is expressed in the cornea, another nonretinal site. Our own preliminary results suggested unpredictably that this photopigment might be localized to nerve fibers coursing throughout the cornea. To verify these initial findings and to test our hypothesis, we examined the corneas of mice in which the melanopsin gene (*Opn4*) drove the expression of fluorescent proteins. We also studied the immunolabeling for melanopsin within the cornea. Both approaches revealed melanopsin expression. However, the neither optical calcium indicator nor patch pipette electrophysiological recordings showed any corneal fiber responses to light. Since many sensory nerve fibers in the cornea originate from neurons in the trigeminal ganglia (TG), we investigated whether melanopsin is expressed in the TG neurons and whether these TG neurons are light sensitive. Melanopsin mRNA was found in the TG, and the fluorescent marker tdTomato from $Opn4^{cre}$::Ai14 mice was also localized in TG neuronal cell bodies. Electrophysiological and calcium indicator measurements failed to show any light responses in the TG neurons. We interpret these findings as evidence that direct photo activation of melanopsin in corneal fibers or in TG neurons plays a very little role, if any, in mediating any type of photoresponses or in acute behavioral photoaversion. These findings raise the possibility that melanopsin may serve nonvisual functions in the cornea.

Materials and methods

Animals

Mice were housed in an AALAC-accredited pathogen-free UCSF animal facility with *ad libitum* access to food and water. The mice were on a 12-h light–dark cycle with lights on at 7 AM and off at 7 PM. The University of California, San Francisco Institutional Animal Care and Use Committee (Animal Welfare Assurance Number: A3400–01) specifically approved the murine component of this study done at UCSF. The University Miguel Hernandez and the Valencian Government approved the experimental protocols for both mice and guinea pigs. The protocols, animal care procedures, and the experimental methods meet all of the guidelines on the care and use of laboratory animals by the U.S. Public Health Service. This study conformed to the ARVO Statement for Use of Animals in Ophthalmic and Vision Research.

The following mouse strains were used in this study: $Opn4^{cre}$ knock in mice with Cre recombinase under the control of the endogenous melanopsin promoter (Ecker et al., 2010); $Opn4^{GFP}$ transgenic mice with the green fluorescent protein gene driven by the melanopsin promoter (Schmidt et al., 2008); Ai14 strain of mice with the floxed tdTomato gene in the rosa26 locus (Madisen et al., 2010); Ai38 strain with the floxed GCaMP3 gene in the rosa26 locus encoding a calcium sensor (Zariwala et al., 2012); C57Bl/6J wild-type mice (Jackson Laboratory, Sacramento, CA); and melanopsin knockout mice (Panda et al., 2003). To trace possible projections from mRGCs into the ciliary body and the iris, which are pigmented

tissues, we developed an albino strain of the *Opn4*^{cre} knock in mice by first crossing these mice with the albino C57 strain (Jackson Laboratory, Sacramento, CA) and then by subsequently breeding the albino progeny into homozygosity for the *Opn4*^{cre} allele.

Adult C57Bl/6J wild-type mice of both sexes and Dunkin Hartley guinea pigs of both sexes were used in this study.

AAV-mediated analysis of melanopsin expression in the eye

Melanopsin-expressing cells in the eyes of adult mice were labeled by intravitreal injection of the Cre-dependent human placental alkaline phosphatase (PLAP) reporter (AAV-flex-plap; Plasmid #80422, Addgene, Cambridge, MA; Delwig et al., 2016). Mice were anesthetized with isoflurane and topical administration of proparacaine (0.5%; Bausch & Lomb). The pupils were dilated by topical administration of phenylephrine (2.5%; Bausch & Lomb) and atropine sulfate (1%; Bausch & Lomb) eye drops. A 32-gauge Hamilton syringe was used to inject 2 μl of the virus into the superior part of the vitreous of the right eye. Two to eight weeks after the intravitreal injection, the mice were euthanized by CO_2 and transcardially perfused with 10 ml HEPES-buffered saline (HBS; 8.2 g/l NaCl, 6 g/l HEPES, 0.1 g/l Na_2HPO_4, pH to 7.4 with NaOH) followed by 20 ml cold 4% paraformaldehyde (PFA) in HBS. All subsequent solutions were prepared with HBS unless otherwise noted. PLAP in the eye tissues was visualized following published protocols (Shah et al., 2004). Briefly, the whole-mount cornea, iris, retina, and sclera were dissected and post-fixed in 4% PFA for 3–4 h at 4°C. Following rinsing in HBS, the endogenous alkaline phosphatase was heat-inactivated by incubation at 72°C for 1 h. Tissue was then washed twice in the buffer A (100 mM Tris pH 7.5, 150 mM NaCl) and then twice again in the buffer B (100 mM Tris pH 9.5, 100 mM NaCl, 50 mM $MgCl_2$). The PLAP reporter was visualized by incubating the tissue in buffer B supplemented with BCIP (0.2 mg/ml) and NBT (1 mg/ml) at room temperature for 1 to 12 h. The PLAP reaction was monitored and stopped before background staining became excessive by rinsing 3 times in 1 mM EDTA followed by postfixation in 4% PFA for 1 h. To remove the background staining, the tissue was cleared by immersing it in ethanol series (30%–70%–95%–100%–95%–70%–30%) for 1–3 min in each concentration and washing subsequently in the HBS. The tissue was mounted on microscope slides, briefly rinsed in distilled water, and cover-slipped using the Aqua/Poly mount (Polysciences, Cat. #18606).

AAV-mediated analysis of melanopsin expression in dissociated, cultured adult murine TG neurons

Neurons from murine trigeminal ganglia were labeled with cre-dependent tdTomato and PLAP reporters (AAV-flex-plap virus, University of North Carolina Virus Vector Core). The TG neurons were isolated and cultured as described previously (Bertke et al., 2011). Briefly, cultures of TG neurons from *Opn4*^{cre}::Ai14 mice were infected with AAV-flex-plap and subsequently processed for PLAP and then visualized two weeks after transduction using the same protocols explained above for intravitreal injections (Shah et al., 2004). For a separate set of experiments examining calcium responses in live cells with the indicator Fura-2, we transfected 2-month-old TG cell cultures from *Opn4*^{cre}::Ai14 mice with the AAV-hSyn-floxed EFGP virus (4 μl; 6×10^{12} titer). The presence of EGFP in cultured neurons verified

with a fluorescent marker that the ongoing melanopsin expression continued in these cultured neurons.

Immunohistochemistry

Adult wild type and melanopsin knockout mice were euthanized in a CO_2 chamber. The corneas were dissected, fixed in 4% PFA overnight at +4°C, and then pretreated with Dent's bleach for 3 h at room temperature (4 parts 100% methanol, 1 part DMSO, 1 part 30% hydrogen peroxide). Following the rehydration series in PBS with 50%–20%–0% methanol (30 min each at room temperature), the corneas were immersed in an antigen blocking solution consisting of PBS with 5% normal goat serum, 1% BSA, and 0.3% TX-100 overnight at +4°C. Subsequent primary and secondary stainings were done in PBS with 1% NGS and 0.1% TX-100. For the primary staining, we used two antimelanopsin antibodies: (1) UF008, Advanced Targeting Systems (http://antibodyregistry.org/search?q=uf008) at 1:5000 for 3 days at +4°C; and (2) an affinity purified rabbit antimelanopsin polyclonal antibody raised against the first 15 amino acids of the N-terminus of melanopsin (Tu et al., 2005). Secondary, tertiary, and DAB stainings were done as previously described (Delwig et al., 2016).

All images were processed using Adobe Photoshop software (Adobe, San Jose, CA).

Analysis of mRNA expression

Mouse tissue was dissected in ice-cold PBS and transferred directly into 1.5 ml Eppendorf tubes filled with 100 μl of Trizol (Invitrogen, Cat. No. 15596–026 Waltham, NY). The collected tissue was homogenized and then lysed in 1 ml of Trizol. RNA extraction was performed according to the manufacturer's protocol. Briefly, RNA was separated into the aqueous phase by addition of 200 μl chloroform followed by vigorous mixing and centrifugation at +4°C at 16,100*g* for 15 min. The aqueous phase was transferred to a new 1.5 ml Eppendorf tube, and RNA was precipitated by addition of 500 μl 100% isopropanol followed by 10 min of incubation at room temperature and centrifugation at +4°C at 16,100*g* for 15 min. The resulting RNA pellet was washed in 75% ethanol and dissolved in DEPC-treated water at +55°C for 10 min. Aspiration in all steps was performed with a drawn-out Pasteur glass pipette. Concentration of RNA was measured using a Nanodrop® ND-100 spectrophotometer (NanoDrop, Wilmington, DE). RNA from the lysates was treated with a Turbo DNA-free Kit (Ambion, Cat. No. AM1907 Waltham, NY) to remove any contaminating DNA. cDNA was generated by reverse transcribing 1 μg of RNA with SuperScript III Reverse Transcriptase (Invitrogen, Cat. No. 18080–093) and oligo (dT) primers. Expressed genes were determined by polymerase chain reaction (PCR) analysis of the cDNA using Platinum Taq DNA polymerase (Invitrogen, Cat. No. 11304–011). PCR primers were manually designed to amplify the ~500 bp fragment of the melanopsin cDNA spanning exons 1 through 4 (5′-CCG CAG GGT TAA GGA TGG TAT-3′,5′-GCA TAG AAC TCG CAA CCT GT-3′) and exons 4 through 8 (5′-CCA AAA GAC GAA CGG CAC TC-3′,5′-GCC TGA TAC ACC GAG AAG CA-3′). The expected product sizes, respectively, are 524 and 575 bp for cDNA and 2856 and 3127 bp for genomic DNA. As a positive control of the RT-PCR, we used primers for mouse beta-actin (5′-ACA GGA TGC AGA AGG AGA TTA C-3′,5′-GTG TAA AAC GCA GCT CAG TAA C-3′). Primers were

validated by the identification of single PCR products of the correct size on agarose gel and direct DNA sequencing.

Electrophysiological recordings of nerve impulse activity in guinea pig and mouse corneas

Nerve impulse activity of peripheral corneal receptor terminals was recorded in isolated eyes or in surgically isolated, superfused cornea preparations (Brock et al., 1998; Parra et al., 2010; Kovács et al., 2016; González-González et al., 2017). In brief, animals were killed with an intraperitoneal injection of 100-mg/kg sodium pentobarbitone, and both corneas were immediately excised and continuously perfused with a physiological solution (composition in mM: 133.4 NaCl; 4.7 KCl; 2 $CaCl_2$; 1.2 $MgCl_2$; 16.3 $NaHCO_3$; 1.3 NaH_2PO_4; and 9.8 glucose; gassed with carbogen: 95% O_2, 5% CO_2 to pH 7.4) at room temperature.

Guinea pig superfused cornea preparation

Cold thermoreceptor terminals were recorded by cutting corneas circularly at the limbus, placing them in a perfusion chamber, and securing them with insect pins inserted into the silicone bottom of the chamber. Corneas were continuously perfused with the physiological solution described above and maintained at 34°C (basal temperature) by means of a feedback-regulated, homemade Peltier device that allowed decreases in the bath temperature from 34°C to 15°C at a constant rate (cooling ramp). The activity of single-cold thermoreceptor terminals was recorded using glass micropipette electrodes (50–100 μm tip diameter) filled with a bath saline solution and applied onto the surface of the cornea using slight suction. The electrical signals were measured with respect to an Ag/AgCl pellet in the bath. Electrical activity was amplified (AC preamplifier NL 103; Digitimer, Welwyn, UK), filtered (high pass cutoff at 5 KHz, low pass cutoff at 150 Hz; filter module NL 125; Digitimer), transferred at 20 KHz to a PC with a CED micro-1401 mk II acquisition system (Cambridge Electronic Design, Cambridge, UK), and analyzed with the indicated software (Spike 2 software v8.0; also from Cambridge Electronic Design).

During the search for an active unit in the isolated cornea preparation, illumination was provided by a Volpi light source (Volpi Intralux 5000–1, Volpi AG, Schlieren, Switzerland), with the fiber optic beam directed obliquely to the corneal surface. Cold thermoreceptor terminals were identified by their continuous, regular ongoing discharge of Nerve Terminal Impulses (NTIs) at 34°C, which increased markedly in response to a cooling ramp down to 15°C (Fig. 4). After a cold unit was obtained and identified, the light was turned off and the cornea was maintained at 34°C in complete darkness for 5 min. Then, a white light beam of maximal intensity (~0.02 W/cm^2 was directed for 3 min to the corneal area, where the recording electrode was placed. Finally, the recording was continued in darkness for another 5 min.

Guinea pig excised eye preparation

To record polymodal nociceptor axons in guinea pig cornea, the excised eye preparation was used. The excised eye was placed in a double compartment chamber. In the front part of the chamber, the conjunctiva was pinned to the separating wall. The compartment containing the

cornea was perfused with warm saline (34°C) dropping continuously over the upper corneal/scleral border. In the rear compartment of the chamber, filled with warmed mineral oil, nerve filaments were teased apart from the ciliary nerves and placed on an Ag–AgCl electrode for the monopolar recording of a single-unit impulse activity, using conventional electrophysiological equipment (gain 310,000, high-pass 300 Hz, low-pass 3 KHz; DAM50 amplifier; WPI, Sarasota, FL). Electrical activity was stored in a computer, using a CED interface (CED micro1401 mk II; Cambridge Electronic Design, Cambridge, United Kingdom) and Spike 2 software (v8.0, also from CED).

In the isolated eye preparation, the ciliary nerve bundles containing touch sensitive fibers were identified and localized by touching the corneal receptive area with a wet brush. By successive splitting under the microscope, a filament containing a single identifiable unit was then isolated. Polymodal nociceptor units were characterized by their response to mechanical stimulus within their receptive area in the cornea using a von Frey filament and to chemical stimulation with a gas jet containing 98.5% CO_2, applied to the corneal receptive field for 30 s. After characterization, the 5 min dark, 3 min light, and 5 min dark protocol was performed, as described above.

Mouse excised eye preparation

The excised eyes were placed in a recording chamber with the posterior pole of the eyeball and the optic nerve introduced into a silicone tube filled with a saline solution located at the bottom of the chamber, where continuous suction is applied to secure the eyeball in place. The eyes were continuously superfused with a physiological saline solution of the following composition (in mM): NaCl (128), KCl (5), NaH_2PO_4 (1), $NaHCO_3$ (26), $CaCl_2$ (2.4), $MgCl_2$ (1.3), and glucose (10), gassed with carbogen to obtain pH 7.4. Temperature of the perfusion solution was maintained at the basal temperature (34°C) with a homemade Peltier device. Borosilicate glass micropipette electrodes (tip diameter of about 50 μm) filled with a saline solution were gently placed against the corneal surface using a micromanipulator, and light suction was then applied through the pipette to produce a high-resistance seal with the corneal surface. Nerve terminal impulses generated at single nerve terminals located beneath the electrode tip were amplified, recorded, and analyzed as described above for the guinea pig experiments. After characterization of the recorded unit, the dark-light-dark protocol was performed as stated above.

Using the calcium indicator GCaMP3 to test for light responses in retina and cornea

We used a genetic method to express the intracellular calcium indicator protein' GCaMP3 in melanopsin cells. The *Ai38* mouse strain that expresses floxed GCaMP3 (B6; 129S-Gt (ROSA) 26Sortm38(CAG-GCaMP3)Hze/J) was obtained from the Jackson Laboratory. We examined retinas and corneas from *Opn4*$^{cre/+}$::Ai38 and *Opn4*$^{cre/-}$::*Ai*38 (melanopsin null) pups. All experimental animals were genotyped. Retinas and the surrounding eye tissue from *Opn4*^{cre}::Ai38 (*floxed GCaMP3*) the albino mice were dissected such that the peripheral retina/ciliary margin remained attached to the sclera and cornea. There was no pigment from the RPE or iris to block the fluorescent signal. Epifluorescence generated by GCaMP3 was imaged in an inverted Nikon (TE2000S) microscope (20 × S-Fluor objective, NA 0.75 Carl Zeiss Microscopy, Thornwood, NY). Stimulation light was provided by a 175-Watt Xenon

Arc lamp (Lambda LS) Stand-Alone Xenon Arc Lamp and Power Supply (Sutter Instruments, Novato, CA). Incident light passed through a FITC/TRITC filter set (Chroma Technology Corp. 51004v2—Peak excitation wavelength 480 nm, Bellows Falls, VT). Fluorescence was imaged onto a CCD camera (Hamamatsu Orca Flash 4.0 LT, Sunnyvale, CA (C11440; 2048 × 2048 pixels). The field of view was ~660 μm × 660 μm. Images were acquired using 4 × 4 binning and had resulting resolution of 512 × 512 pixels. Excitation light simultaneously activated GCaMP3 and stimulated melanopsin photopigment. Light stimuli were presented at 2 Hz and 3 Hz. Stimulation/acquisition periods were 530 ms (2 Hz) and 330 ms (3 Hz). Regions of interest encircling somas of GCaMP3 fluorescent cells were set manually on images recorded from the best-focused position. Fluorescent images from complete fields of view were recorded continuously. Summed responses from all pixels within each ROI were also viewed in real time and recorded to the disc. Photo bleaching of GCaMP3 was deemed minimal. We could directly assess GCaMP3 photo bleaching in melanopsin knockout mice, (*OPN4*$^{cre/-}$::Ai38). At the termination of the stimulus, $\Delta F/F$ remained within 97% of that at the onset of the stimulus (data not shown).

Using the calcium indicator Fura-2 to test for light responses in TG neurons

We transfected 2-month-old TG cell cultures from *Opn4*^{cre}::Ai14 mice with AAV-hSvn-floxed EFGP virus (4 μl; 6 × 10^{12} titer). The presence of EGFP in cultured neurons verified with a fluorescent marker whether the ongoing melanopsin expression continued in these cultured neurons. TG cells adhering to 5 mm round cover-slips were covered with a meniscal bubble of ACSF solution at RT. A 5-μl aliquot of 1 mM Fura-2 AM and 5 μl of 20% pluronic acid (F127) were dropped into the bubble. The coverslips were kept at RT for 1 h and then transferred into a perfusion chamber mounted on the stage of a Nikon inverted microscope (see above description for GCaMP3 measurements). Intracellular calcium was monitored by obtaining fluorescent emission from individual cells alternately flashed with 340 nm and 380 nm excitation lights through the optics of the microscope. We used standard ratiometric values to quantify relative calcium concentrations over time (Krizaj & Copenhagen, 1998; Hartwick et al., 2007; Jo et al., 2015).

In the Fura-2 experiments, we were unable to record changes in fluorescence when the stimulation light was on. The calcium off rate for Fura-2 is ~85 s^{-1} (Jackson et al., 1987). Hence, even though the data could not be collected during the period of stimulation, this slow off rate allowed us to easily monitor the decay phase of any light responses.

Results

Genetic marking techniques reveal melanopsin in cornea

The dendritic arbors, cell bodies, and axons of melanopsin ganglion cells (mRGCs) in the retina can be elegantly visualized using a cre/lox system to express the loxP flanked marker genes. Commonly, melanopsin cre mice (*Opn4*^{cre}) are mated with cre-dependent reporter lines to generate alkaline phosphatase or the fluorescent protein EGFP within the melanopsin ganglion cells in the retina (mRGCs) (Berson et al., 2010; Ecker et al., 2010). As part of our other ongoing studies examining the morphology of mRGCs, we used *Opn4*^{cre}::Ai14 mice to study the expression of the bright fluorescent protein tdTomato in

mRGCs. Unexpectedly, when examining the far peripheral regions of the retina, we discovered the melanopsin cell marker tdTomato in the fibers within the cornea (Fig. 1A–1D). Fig. 1A and 1B show tdTomato-filled fibers in corneas of two different mice. Fig. 1C and 1D show examples of lobular structures that are probably terminal fields of nerve fibers in the epithelium (Ohara et al., 2000). Supplementary material Fig. 1, a low-magnification, montage image of an entire flat mounted cornea, reveals tdTomato fibers that enter from the edge of the cornea and arborize within the cornea.

While these findings appear to indicate heretofore unreported melanopsin expression in the cornea, one caveat of using this cre/lox approach is the possibility that the tdTomato expression was initiated at an earlier age and persisted in the cornea after the melanopsin transcription had ceased. In an attempt to validate the tdTomato corneal results and to determine whether melanopsin was being actively expressed in the corneas of adult mice, we injected an adeno-associated virus (AAV) with the floxed human placental alkaline phosphatase (PLAP) gene (AAV-flex-plap) into the vitreal cavity of *Opn4*^{cre} mice (Delwig et al., 2016). The rationale for this approach is that the PLAP would only be observed in those cells that were both acutely transduced by the intraocularly injected AAV-flex-plap and were simultaneously expressing *Opn4*^{cre}. We readily observed PLAP staining in the retinas (Delwig et al., 2016) and in the corneas and anterior regions of the injected eyes. We saw prominent PLAP staining in both the nerves in the cornea (Fig. 1E) and the dendritic-like cells at the level of the corneal endothelium (inset in the Fig. 1E). These findings can be interpreted as evidence that cell bodies that extend fibers into the cornea were indeed actively expressing the melanopsin gene. This discovery suggests that some mRGCs within the retina might be the source of cells that project fibers into the cornea. We confirmed a rich plexus of mRGCs in the peripheral retina (Semo et al., 2010, Supplementary material Fig. 2). These mRGCs might have projected their processes into the cornea; however, we failed to see fibers extending past the ciliary body. Alternatively, PLAP staining in the cornea might reflect AAV that had diffused into the anterior chamber and infected the cells in the cornea, or alternatively, some of the virus escaped from the injection site and infected nearby nerve fibers, such as fibers from the trigeminal ganglia, that innervate the cornea.

An alternative noncre/lox approach confirmed the presence of the melanopsin-driven reporter in corneal fibers. We examined corneas of the *Opn4*^{GFP} transgenic strain of mice. Fig. 1F shows an example of multiple GFP-positive fibers running across the sclera in these mice. We commonly observed GFP-positive fibers entering the cornea from the sclera. In some instances, we found evidence of GFP-positive lobular structures often seemingly connected to nearby individual fibers (data not shown). Taken together, these data, generated form two different genetic approaches, suggest that melanopsin is present in the cornea.

Melanopsin-specific antibodies show melanopsin protein in the cornea

To detect directly the presence of the melanopsin protein in the cornea, we performed immunolabeling of flat mounted mouse corneas. Using two independent antibodies against mouse melanopsin, we were able to detect immunostaining in the cornea. Fig. 2 shows examples of melanopsin immunoreactivity in the epithelial (Fig. 2A and 2B) and endothelial layers (Fig. 2C and 2D), respectively. Immunoreactivity was localized to sparse fibers in the

cor-neal stroma/epithelium and to dendritic-like cells at the level of the corneal endothelium. Control experiments in melanopsin-knockout mice failed to detect any labeling (Fig. 2B and 2D). Thus, both genetically driven markers and antibody staining strongly support the existence of the melanopsin expression in the corneas of mice.

Trigeminal origin of the melanopsin-positive fibers in the cornea

Since most nerve fibers in the cornea originate in the trigeminal ganglia (TG), we tested the parsimonious explanation that the presence of melanopsin in corneal fibers reflected its expression in a subset of neuronal cell bodies in the ophthalmic division (V1) of the TG. Fibers from the V1 region of TG provide somatic sensory innervation to the upper face, cranium, and eyes, including the cornea. In the cornea, specialized receptors on these fiber endings respond to “nociceptive” stimuli including pressure, temperature, and capsaicin.

RT-PCR analysis of the retina and TG neurons revealed evidence of melanopsin mRNA. The left panel in Fig. 3A shows prominent PCR bands from the retina, each of which contains 2000–3000 melanopsin ganglion cells (Berson et al., 2010; Valiente-Soriano et al., 2014). Bands for melanopsin were observed in TG neuron preparations. The bands identified in the TG required five additional PCR cycles than retina, suggesting that the density of melanopsin positive neurons was significantly lower than that in the retina. We also ran RT-PCR on the isolated corneal tissue. We failed to detect any melanopsin mRNA in the cornea. This finding ruled out the possibility that the melanopsin protein synthesis might be occurring from mRNA within the corneal fibers themselves (Hanus and Schuman 2013) rather than in the TG neuronal cell bodies.

In the V1 region of the TG in *Opn4*^{cre}::Ai14 mice we found tdTomato labeling in a subset of sensory neurons (Fig. 3B). This finding supports the idea of the melanopsin expression in the TG neurons and confirms an earlier report using *Opn4*^{EGFP} mice (Matynia et al., 2016). However, as mentioned above, because the tdTomato labeling in *Opn4*^{cre}::Ai14 mice can reflect the historical activity of the *Opn4* promoter; we sought to determine if the *Opn4* promoter is active in adult mice. To address this concern, we infected primary neuronal cultures harvested from the TG of *Opn4*^{cre} mice with the AAV-flex-plap. Similar to tdTomato genetic reporter expression (Fig. 3B) and consistent with the melanopsin mRNA expression (Fig. 3A), we found the PLAP reporter signal in a subset of TG neurons (Fig. 3C), pointing to active transcription in the adult. In spite of finding a genetic signature for melanopsin in TG, we were unable to show the specific labeling of TG neurons using either of the melanopsin antibodies. Both of the melanopsin antibodies tested in TG cultures exhibited nonspecific binding making it problematical to identify specific melanopsin protein expression. Matynia et al. (2016) did show melanopsin immunoreactivity in human TGs but did not show or describe melanopsin immunoreactivity in the mouse TG. In summary, similar to Matynia et al. (2016), we found genetic evidence of melanopsin transcription in a subset of mouse TG neurons but failed to see evidence for protein expression.

Optical and electrophysiological recordings failed to reveal any light responsive cells or fibers in the cornea

We explored whether the melanopsin expression in the cornea imbued fibers with intrinsic photosensitivity. We first used optical imaging of cells expressing a calcium indicator protein to detect light-evoked activity in the melanopsin-expressing fibers in the cornea. We examined corneas harvested from *Opn4*^{cre}::Ai38 mice that express the GCaMP3 calcium indicator in melanopsin cells. We tested for light-induced calcium in GCaMP3-labeled cells in the cornea and also tested for responses in GCaMP3-labeled nerve trunks entering the cornea from the limbus. Tissue pieces from the anterior segments of *Opn4*^{cre}::Ai38 albino mice were dissected such that the peripheral retina and ciliary margin remained attached to the sclera and cornea. These tissue pieces were flat mounted and placed into a perfusion chamber above the objective of an inverted microscope (see Materials and methods). There was no pigment in the RPE or iris to block the fluorescent signal as these animals were bred on an albino background strain. The calcium responses for four selected regions of interest in both the cornea near the scleral edge (Fig. 4A–4C) and in the retina near the ciliary margin (Fig. 4D–4F) are shown. The regions observed in the cornea did not show a light-evoked change in intracellular calcium above the baseline fluorescence (A). Actual fluorescent images of the cornea that includes cells plotted in (A) are shown in successive frames at 0 and 3 s (B and C). In contrast, many cells, which correspond to mRGCs in the peripheral retina, exhibited light-dependent calcium responses (Fig. 4D). These cells were in the peripheral retina that remained attached to our corneal preparations (Fig. 4G and 4H). The time courses of four randomly selected cells exhibiting light responses in the retina are plotted and show an average peak response of about 3 s. Actual fluorescent images, which include cells plotted in (D), are shown in successive frames at 0 and 3 s (E and F).

In other experiments, we imaged GCaMP3 positive bundles of nerves entering the cornea from the limbus. We never were able to observe light-evoked calcium elevations in these fibers ($N > 15$, data not shown). Capsaicin, an agonist for the TRPV1 receptors in trigeminal nerves, and a depolarizing concentration of KCl did elevate calcium in these bundles ($n = 15$ capsaicin, $n = 4$, KCL). In summary, these experiments failed to show light responses in presumed melanopsin-expressing fibers within the cornea or in presumed TG fiber bundles entering the cornea. Our inability to observe calcium responses in the cornea is particularly compelling because we were able to show robust light-evoked responses in the adjacent retina from the same eye recorded under identical conditions.

In another set of experiments, we attempted to detect light-evoked responses electrophysiologically by recording from individual corneal sensory fibers. We were not able to detect light-evoked responses in corneal cold thermoreceptive TG fibers in either the guinea pig or mouse corneas. Guinea pig experiments were performed on five well-recorded, stable cold sensitive nerve terminals of four corneas. The mean NTI frequency at 34°C during a 5-min period measured in the dark was 9.8 ± 0.3 NTI s^{-1} ($n = 5$). Three minutes of exposure to intense light produced an NTI of 9.4 ± 0.4 NTI s^{-1} ($n = 5$), a value virtually identical to the dark. Likewise, when the light was turned off and the mean nerve terminal impulse frequency at 34°C was measured during the following 5 min of darkness, the mean firing frequency was 9.5 ± 0.2 NTI s^{-1} (Fig. 5A). In one cold thermoreceptor unit,

illumination was repeated a second time; the mean firing frequency during this second light stimulus was 8.9 NTI s^{-1}, identical to the mean value in the previous dark period (Fig. 5C). Thus, we found no evidence for light activation of the thermosensitive corneal fibers or for light modulating the responses in these thermosensitive neurons. Similar negative results were obtained from 2 out of 2 polymodal nociceptor units recorded in superfused guinea pig eyes (data not shown).

The effect of light on the nerve terminal impulse activity in the mouse cornea was tested in eight cold sensitive nerve terminals and one polymodal terminal of four corneas. The NTI activity recorded at basal temperature (34°C) in mice corneas was lower than that in guinea pig corneas (4.0 ± 0.6 NTI s^{-1} *vs.* 9.8 ± 0.3 NTI s^{-1} in mice and guinea pigs respectively; $P < 0.001$, *t*-test). Fig. 5B shows a sample recording of the nerve terminal impulse (NTI) activity of a cold thermoreceptor terminal in response to a cooling ramp (from 34 to 20°C) recorded in a mouse cornea. Firing patterns of cold sensitive nerve terminals were not modified during the dark-light-dark protocol (Fig. 5D). The mean NTI activity of mice cold sensitive nerve terminals did not change during the dark-light-dark protocol (4.0 ± 0.6 NTI s^{-1}, 3.9 ± 0.7 NTI s^{-1} and 3.8 ± 0.7 NTI s^{-1} for dark, light, and dark periods, respectively, $n = 8$; $P = 0.535$, One Way ANOVA repeated measures). Thus, these results fail to support the hypothesis that fibers within the cornea are activated by light.

No evidence for light responses in TG neurons

We also failed to find any physiological evidence of light-evoked activity in the TG cell bodies. We used two different independent approaches to detect light-evoked responses in tdTomato-positive TG neurons cultured from *Opn4*^{cre}::Ai14 mice. Searching for light-evoked calcium responses, we surveyed three coverslips containing a total of more than 30 cells expressing *Opn4*^{cre} driven tdTomato and loaded acutely with Fura-2 AM. We failed to observe light-induced calcium increases using Fura-2 but did see KCl-induced calcium elevations in the tdTomato positive TG neurons (data not shown). One caveat of these experiments is that even though tdTomato was expressed, the melanopsin expression may have ceased by the time we tested the cells after two months in culture. To test this possibility, we transfected the 2-month-old TG cell cultures from *Opn4*^{cre}::Ai14 mice with the AAV-hSvn-floxed EFGP virus (4 μl; 6×10^{12} titer). The premise of this method was that, if cells were positive for EGFP, this would show that melanopsin was being actively expressed. Two to three weeks after viral infection, cells on the coverslips were loaded with Fura-2 AM by incubation for 1 h at RT. Coverslips were individually placed in the perfusion chamber for imaging. We first localized EGFP positive cells that showed Fura-2 fluorescence and assumed these would be neurons actively expressing melanopsin. Other neurons on the coverslips were Fura-2 positive and EGFP negative corresponding to other types of nonmelanopsin expressing TG neurons. We compared the responses to elevated potassium (50 mM in isotonic saline). Both the Fura-2 loaded and EGFP plus Fura-2 loaded cells responded with a KCl-induced robust calcium elevation (Fig. 6). No signal was observed in the background region of interest (ROI). None of the TG neurons responded to light. These TG neurons included those loaded with Fura-2 but showing no EGFP fluorescence, presumed to be a nonmelanopsin neuron, and those cells loaded with Fura-2 and show EGFP fluorescence, presumed to be melanopsin-expressing neurons.

We also used an electrophysiological approach to search for light responsive tdTomato cultured TG neurons. Using loose-patch pipettes (Sexton et al., 2015), we found no light-evoked responses in a survey of 17 successfully patched, tdTomato-labeled cultured TG cells. Ten of these recorded cells were depolarized by bath-perfused KCl indicating that these neurons remained viable (data not shown). In summary, these calcium imaging and electrophysiological findings failed to replicate a previous report concluding that TG neurons can be intrinsically photosensitive (Matynia et al., 2016).

Discussion

In this present study, we show that melanopsin markers are expressed in the cornea. The expression is mostly localized to fibers and lobular endings, presumably at the expansions of nerve fibers invading the extracellular spaces in the epithelial layer of the cornea. We also present evidence that melanopsin is expressed in the trigeminal ganglion neurons. Our working conclusion is that a small number of melanopsin-containing fibers from the trigeminal ganglion may extend into the cornea. Although there are caveats to our findings (discussed below), our results are consistent with the hypothesis that melanopsin expressed by TG cell bodies and fibers does not impart photosensitivity to these neurons. The functional significance of the melanopsin expression in the TG or cornea remains unknown.

If melanopsin-expressing trigeminal sensory neurons in the cornea had responded to light, this would have provided an appealing explanation for a possible mechanism of light-induced discomfort in multiple ocular and neurological disorders such as corneal abrasions and intraocular inflammation. This idea had been suggested by Digre and Brennan (2012) who posited that photophobia could be initiated by light striking melanopsin-expressing nerve cells in the anterior region of the eye. Our experiments argue against the notion that light activation of melanopsin fibers in the cornea could be the origin of photophobia initiated in the anterior eye. As an alternative mechanism for photophobia, Digre and Brennan (2012) noted evidence that mRGCs in the peripheral retinal extend their processes intraocularly toward the anterior regions of the eye, which we confirm (Supplementary material Fig. 2). Digre and Brennan suggested that mRGCs could directly activate TG fibers that invade the ciliary body or iris. Intraocular inflammation and corneal lesions *via* the axonal reflex are known to sensitize the iris and the ciliary body (Walsh, 1982; Duane et al., 2013). It is possible that under these pathological coninserditions, light evokes pain *via* direct signaling from mRGCs to the trigeminal sensory nerves inner-vating the ciliary body, inducing the pain associated with the ciliary spasm. Animal studies support this hypothesis. Dolgonos et al. (2011) reported that light directly potentiates the trigeminal blink reflex in rat eyes with lesioned optic nerves. This finding, if confirmed, would be consistent with transmission of visual signals *via* TG pathways that do not exit the eye in the optic nerve.

Three issues need to be considered with regard to our study and the conclusions that can be drawn. First, could the nonoptimal experimental conditions prevent us from observing light responses? Secondly, could light activation of melanopsin be driving a signaling pathway undetectable by our techniques? Third, could melanopsin function as a nonvisual sensory receptor?

Suboptimal experimental conditions could have prevented us from recording light responses. While the corneal fiber recordings were made in freshly harvested tissue, cells in the long-term TG cultures may have lost important components of transduction even though we did test for the melanopsin expression in the older cultures. Perhaps, these cultured TG neurons exhibited a depleted chromophore or rundown of light-sensitive ion channels. Alternatively, it is conceivable that the TG cells and fibers may have a very high threshold to light, so we simply could not activate transduction. However, we used light intensities above 10^{16} photons/cm^2/s that is adequate to stimulate melanopsin-containing cells in the iris and in the retina, so we do not think we are stimulating with inadequate photon fluxes. Our inability to record light responses may also reflect a need for these corneal fibers to be initially sensitized by an injury that induces inflammation or by postinjury remodeling (e.g., LASIK-induced corneal nerve changes) in order to be activated by light (Rosenthal et al., 2009).

If light activated melanopsin drove a signaling pathway that did not elevate intracellular calcium, either by not activating membrane calcium channel or intracellular calcium, we may have not been able to monitor melanopsin activation. This same reasoning applies to signaling pathways that do not modulate voltage-activated ion channels. Another consideration is that light-activated melanopsin is coupled to gene regulation. Light can regulate gene transcription in bacteria, yeast, and plants (Kozma-Bognar et al., 2012; Liu and Zhong 2017).

There is precedent that melanopsin can function as an alternative sensory receptor. *Drosophila* larvae will migrate to a preferred temperature when placed on a substrate having a temperature gradient. This temperature discrimination is lost in the larvae in which the visual pigment rhodopsin is deleted genetically from photoreceptors. Unexpectedly, the melanopsin expression in the photoreceptor cells lacking rhodopsin restores the temperature discrimination (Shen et al., 2011). Whether melanopsin can perform nonvisual functions raises the question of whether its expression in the cornea might serve other sensory modalities.

Supplementary Material

Refer to Web version on PubMed Central for supplementary material.

Acknowledgments

We thank Aye Aye Ma, Peter O'Hare, Kerui Gong, Sebastian Espinoza, Alan Basbaum, Peter Goadsby, Margarida Martins Oliveira, and Laura Cammas for technical help. We are particularly indebted to the late Doug Yasumura for doing the intraocular injections, and to Carlos Belmonte for valuable discussion and agreeing to orchestrate recordings from corneal fibers.

Supported by National Institutes of Health Grants R01 EY 01869, R01 EY023179, T32 EY007120, R21 EY025435, P30 EY002162, EY022697, and F32 EY02114. Additional support was provided by That Man May See (San Francisco), Benign Essential Blepharospasm Research Foundation and Unrestricted Grants from Research to Prevent Blindness (UCSF, UW).

References

Berson DM, Castrucci AM & Provencio I (2010). Morphology and mosaics of melanopsin-expressing retinal ganglion cell types in mice. Journal of Comparative Neurology 518, 2405–2422. [PubMed: 20503419]

Bertke AS, Swanson SM, Chen J, Imai Y, Kinchington PR & Margolis TP (2011). A5-positive primary sensory neurons are non-permissive for productive infection with herpes simplex virus 1 *in vitro*. Journal of Virology 85, 6669–6677. [PubMed: 21507969]

Brock JA, McLachlan EM & Belmonte C (1998). Tetrodotoxin-resistant impulses in single nociceptor nerve terminals in Guinea-pig cornea. Journal of Physiology 512, 211–217. [PubMed: 9729630]

Delwig A, Larsen DD, Yasumura D, Yang CF, Shah NM & Copenhagen DR (2016). Retinofugal projections from melanopsin-expressing retinal ganglion cells revealed by intraocular injections of cre-dependent virus. PLos One 11, e0149501. [PubMed: 26895233]

Digre KB & Brennan KC (2012). Shedding light on photophobia. Journal of Neuro-Ophthalmology 32, 68–81. [PubMed: 22330853]

Do MTH & Yau KW (2010). Intrinsically photosensitive retinal ganglion cells. Physiological Reviews 90, 1547–1581. [PubMed: 20959623]

Dolgonos S, Ayyala H & Evinger C (2011). Light-induced trigeminal sensitization without central visual pathways: Another mechanism for photophobia. Investigative Ophthalmology & Visual Science 52, 7852–7858. [PubMed: 21896840]

Duane TD, Tasman W & Jaeger EA (2013). Duane's Ophthalmology. Philadelphia: Wolters Kluwer/ Lippincott Williams & Wilkins.

Ecker JL, Dumitrescu ON, Wong KY, Alam NM, Chen S-K., LeGates T, Renna JM, Prusky GT, Berson DM & Hattar S (2010). Melanopsin-expressing retinal ganglion-cell photoreceptors: Cellular diversity and role in pattern vision. Neuron 67, 49–60. [PubMed: 20624591]

González-González O, Bech F, Gallar J, Merayo-Lloves J & Belmonte C (2017). Functional properties of sensory nerve terminals of the mouse cornea. Investigative Ophthalmology & Visual Science 58, 404–415. [PubMed: 28118665]

Hartwick AT, Bramley JR, Yu J, Stevens KT, Allen CN, Baldridge WH, Sollars PJ, Pickard GE (2007). Light-evoked calcium responses of isolated melanopsin-expressing retinal ganglion cells. Journal of Neuroscience 27, 13468–13480. [PubMed: 18057205]

Hanus C & Schuman EM (2013). Proteostasis in complex dendrites. Nature Reviews Neuroscience 14, 638–648. [PubMed: 23900412]

Jackson AP, Timmerman MP, Bagshaw CR & Ashley CC (1987). The kinetics of calcium binding to fura-2 and indo-1. FEBS Letters 216, 35–39. [PubMed: 3108033]

Jo AO, Ryskamp DA, Phuong TT, Verkman AS, Yarishkin O, MacAulay N & Križaj D (2015). TRPV4 and AQP4 channels synergistically regulate cell volume and calcium homeostasis in retinal Müller glia. Journal of Neuroscience 35, 13525–13537. [PubMed: 26424896]

Kovács I, Luna C, Quirce S, Mizerska K, Callejo G, Riestra A, Fernández-Sánchez L, Meseguer VM, Cuenca N, Merayo-Lloves J, Acosta MC, Gasull X, Belmonte C & Gallar J (2016). Abnormal activity of corneal cold thermoreceptors underlies the unpleasant sensations in dry eye disease. Pain 157, 399–417. [PubMed: 26675826]

Kozma-Bognar L, Hajdu A & Nagy F (2012). Light-regulated gene expression in yeast. Methods in Molecular Biology 813, 187–193. [PubMed: 22083743]

Krizaj D & Copenhagen DR (1998). Compartmentalization of calcium extrusion mechanisms in the outer and inner segments of photoreceptors. Neuron 21, 249–256. [PubMed: 9697868]

Liu X & Zhong S (2017). Interplay between light and plant hormones in the control of arabidopsis seedling chlorophyll biosynthesis. Frontiers of Plant Science 8, 1433.

Lucas RJ (2013). Mammalian inner retinal photoreception. Cell Biology 23, R125–R133.

Madisen L, Zwingman TA, Sunkin SM, Oh SW, Zariwala HA, Gu H, Ng LL, Palmiter RD, Hawrylycz MJ, Jones AR, Lein ES & Zeng H (2010). A robust and high-throughput Cre reporting and characterization system for the whole mouse brain. Nature Neuroscience 13, 133–140. [PubMed: 20023653]

Matynia A, Nguyen E, Sun X, Blixt FW, Parikh S, Kessler J, de Sevilla Muller LP, Habib S, Kim P, Wang ZZ, Rodriquez A, Charles A, Nuseinowitz S, Edvinnson L, Barnes S, Brecha NC & Gorin MB (2016). Peripheral sensory neurons expressing melanopsin respond to light. Frontiers in Neural Circuits 10, 60. [PubMed: 27559310]

Ohara PT, Chin MS & LaVail JH (2000). The spread of herpes simplex virus type 1 from trigeminal neurons to the murine cornea: An immuno-electron microscopy study. Journal of Virology 74, 4776–4786. [PubMed: 10775616]

Panda S, Provencio I, Tu DC, Pires SS, Rollag MD, Castrucci AM, Pletcher MT, Sato TK, Wiltshire T, Andahazy M, Kay SA, Van Gelder RN & Hogenesch JB (2003). Melanopsin is required for non-image-forming photic responses in blind mice. Science 301, 525–527. [PubMed: 12829787]

Parra A, Madrid R, Echevarria D, del Olmo S, Morenilla-Palao C, Acosta MC, Gallar J, Dhaka A, Viana F & Belmonte C (2010). Ocular surface wetness is regulated by TRPM8-dependent cold thermoreceptors of the cornea. Nature Medicine 16, 1396–1399.

Regard JB, Sato IT & Coughlin SR (2008). Anatomical profiling of G-protein-coupled receptor expression. Cell 135, 561–571. [PubMed: 18984166]

Rosenthal P, Baran I & Jacobs DS (2009). Corneal pain without stain: Is it real? Ocular Surface 7, 28–40. [PubMed: 19214350]

Schmidt TM, Taniguchi K & Kofuji P (2008). Intrinsic and extrinsic light responses in melanopsin-expressing ganglion cells during mouse development. Journal of Neurophysiology 100, 371–384. [PubMed: 18480363]

Sexton TJ, Bleckert A, Turner MH & Van Gelder RN (2015). Type I intrinsically photosensitive retinal ganglion cells of early post-natal development correspond to the M4 subtype. Neural Development 10, 17. [PubMed: 26091805]

Semo M, Gias C, Ahmado A, Sugano E, Allen AE, Lawrence JM, Tomita H, Coffey PJ & Vugler AA (2010). Dissecting a role for melanopsin in behavioural light aversion reveals a response independent of conventional photoreception. PloS One 5, e15009. [PubMed: 21124784]

Shah NM, Pisapia DJ, Maniatis S, Mendelsohn MM, Nemes A & Axel R (2004). Visualizing sexual dimorphism in the brain. Neuron 43, 313–319. [PubMed: 15294140]

Shen WL, Kwon Y, Adegbola AA, Luo J, Chess A & Montell C (2011). Function of rhodopsin in temperature discrimination in Drosophila. Science 331, 1333–1336. [PubMed: 21393546]

Sikka G, Berkowitz DE, Hussman GP, Pandey D, Cao S, Hori D, Park JT, Steppan J, Kim JH, Barodka V, Myers AC, Santhanam L, Nyhan D, Halushka MK, Koehler RC, Snyder SH, Shimoda LA & Berkowitz DE (2014). Melanopsin mediates light-dependent relaxation in blood vessels. Proceedings of the National Academy of Sciences of the United States of America 111, 17977–17982. [PubMed: 25404319]

Tu DC, Zhang D, Demas J, Slutsky EB, Provencio I, Holy TE & Van Gelder RN (2005). Physiologic diversity and development of intrinsically photosensitive retinal ganglion cells. Neuron 48, 987–999. [PubMed: 16364902]

Valiente-Soriano FJ, García-Ayuso D, Ortín-Martínez A, Jiménez-López M, Galindo-Romero C, Villegas-Pérez MP, Agudo-Barriuso M, Vugler AA & Vidal-Sanz M (2014). Distribution of melanopsin positive neurons in pigmented and albino mice: Evidence for melanopsin interneurons in the mouse retina. Frontiers in Neuroanatomy 8, 131. [PubMed: 25477787]

Walsh FB (1982). Walsh and Hoyt's Clinical Neuro-ophthalmology (4th ed.), p. 5 Baltimore: Williams & Wilkins.

Xue T, Do MTH, Riccio A, Jiang Z, Hsieh J, Wang HC, Merbs SL, Welsbie DS, Yoshioka T, Weissgerber P, Stolz S, Flockerzi V, Freichel M, Simon MI, Clapham DE & Yau KW (2011). Melanopsin signalling in mammalian iris and retina. Nature 479, 67–73. [PubMed: 22051675]

Zariwala HA, Borghuis BG, Hoogland TM, Madisen L, Tian L, De Zeeuw CI, Zeng H, Looger LL, Svoboda K & Chen TW (2012). A Cre-dependent GCaMP3 reporter mouse for neuronal imaging in vivo. Journal of Neuroscience 32, 3131–3141. [PubMed: 22378886]

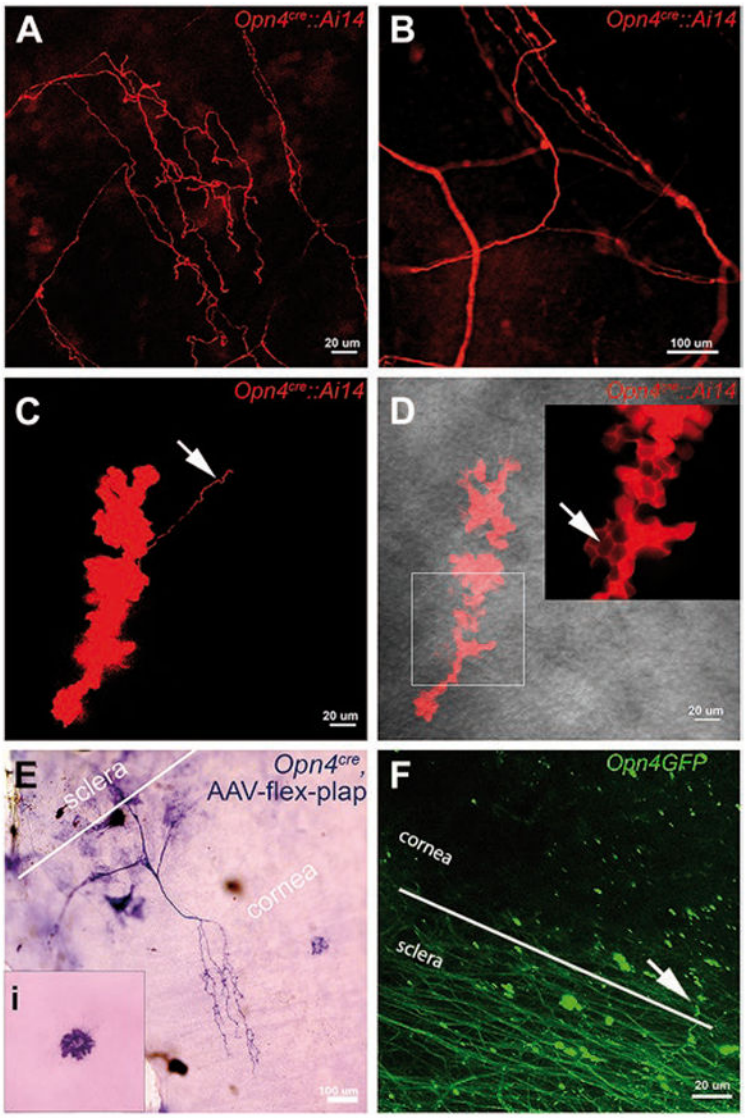

Fig. 1.

Melanopsin expression in cornea revealed by genetically driven markers. (**A**–**D**) Corneal epithelium from adult *Opn4*^{cre}::*Ai*14 mice. Red color shows melanopsin-driven tdTomato reporter. (**A**) Confocal imaging in stromal layer of the cornea reveals a network of tdTomato-positive fibers. (**B**) Small area of tdTomato filled fibers across cornea of another *Opn4*^{cre}::*Ai*14 mouse. This figure is an expanded view of the square outlined in Sup. Fig. 1. Image captured between the epithelial and stromal layers reveals bulbous “clump” of cells. Arrow points to a fiber emanating from the clump. (**D**) tdTomato staining reveals bulbous terminal ending in more superficial layer of cornea than shown in (**C**). Arrow in the insert denotes localization of tdTomato in the intra-epithelial spaces. Gray background shows bright field view of the corneal epithelium. (**E**) The cornea from an *Opn4*^{cre} mouse that received an intravitreal injection of AAV-flex-plap shows the expression of PLAP in the nerve fibers and dendritic-like cells at the level of the corneal endothelium (inset). (**F**) GFP-positive fibers in sclera and cornea in an *Opn4*^{GFP} mouse. Scale bars are marked.

Comparable findings for all genetic approaches mentioned above were found in 4 to 10 mice across at least 3 litters.

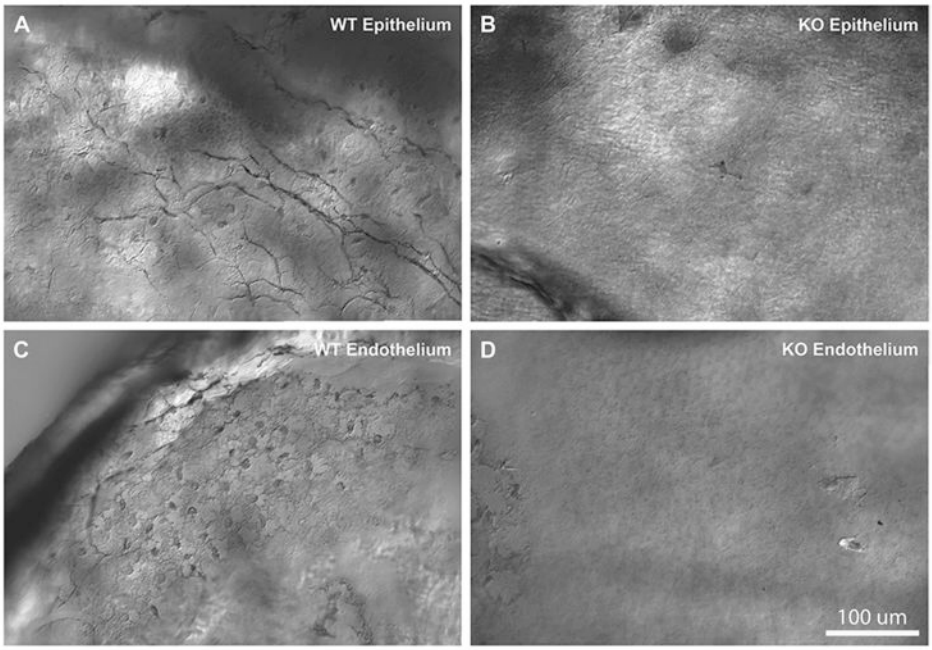

Fig. 2.

Melanopsin expression in the cornea revealed by the melanopsin-specific antibody, immunostaining of the mouse cornea with the antimelanopsin antibody made in the lab (see Materials and methods). Images obtained in corneal epithelium (**A**, **B**) and near the endothelium (**C**, **D**). Panels include comparisons of immunoreactivity in melanopsin wildtype mice (**A**, **C**) and knockout mice (**B**, **D**). Melanopsin staining in WT mice demonstrated immunoreactive fibers in the epithelial part of the cornea, and fibers and round structures, putative dendritic or endothelial cells, near the endothelial surface. No immunoreactive fibers or cells were detected in the melanopsin knockout mice. Similar findings were obtained in at least 4 different WT and melanopsin knockout mice.

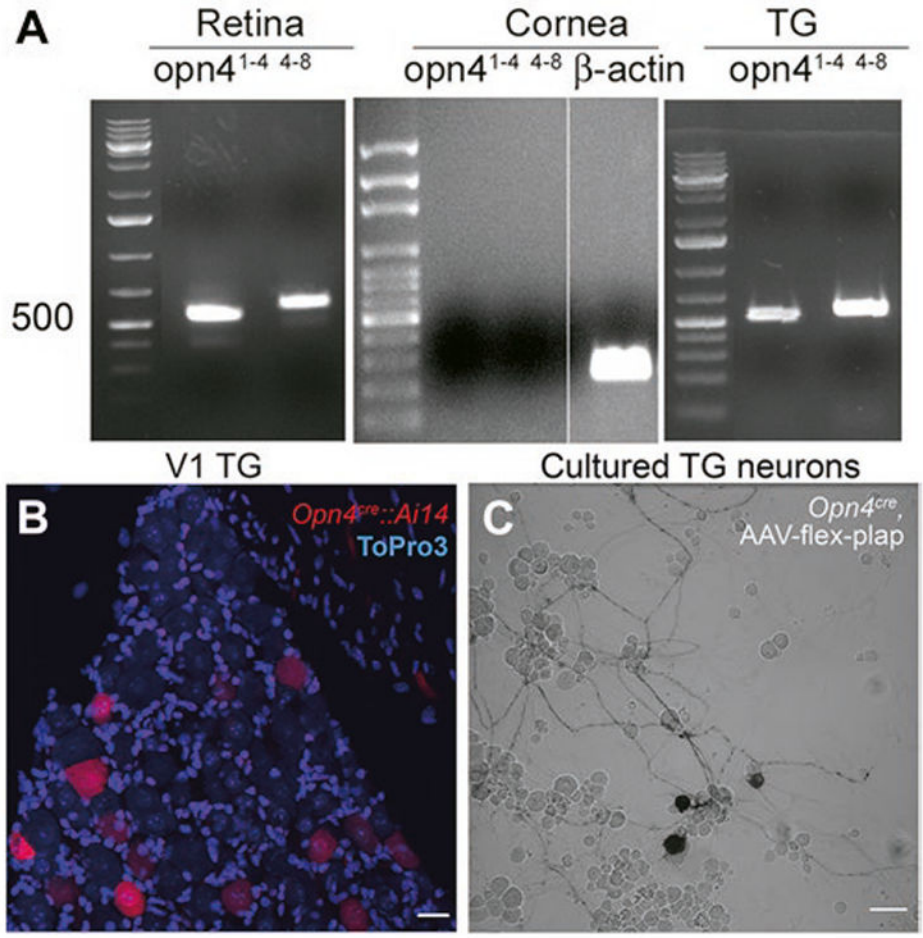

Fig. 3.

Melanopsin mRNA is detected in retina and trigeminal ganglia but not in cornea. Melanopsin-driven markers can be observed in cells imaged in whole-mounted trigeminal ganglia and in culture. (**A**) RT-PCR results illustrates the expression of the melanopsin mRNA in the retina and the trigeminal ganglion (TG) but not the cornea. The melanopsin expression was probed with two sets of primers encompassing exons 1 through 4 (superscript 1–4) and exons 4 through 8 (superscript 4–8). (**B**) V1 part of the trigeminal ganglion from *Opn4*^{cre}::Ai14 mouse (P98). Red color shows Ai14 reporter; blue color shows nuclei of cells (ToPro3 stain). Scale bar: 20 μm. (**C**) Neuronal culture from the trigeminal ganglion of the *Opn4*^{cre} mouse infected with the AAV-flex-plap. Black color shows the expression of PLAP. Scale bar: 50 μm. Each PCR result was obtained in no fewer than three mice.

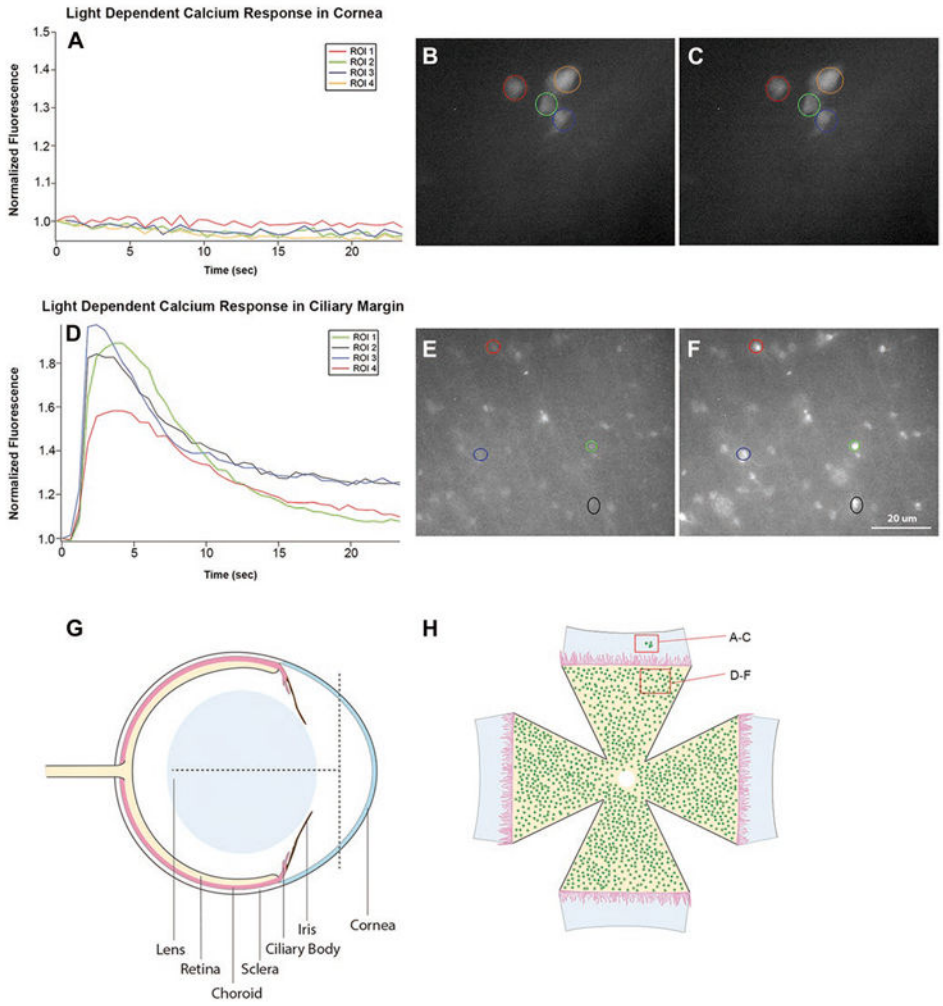

Fig. 4.

Light evokes responses in melanopsin cells of retina but not in the adjacent melanopsin expressing cells within the cornea. Retinas and surrounding tissue from *Opn4*^{cre}::Ai38 (flox) albino mice were dissected such that the peripheral retina/ciliary margin remained attached to the sclera and cornea. There was no pigment from the RPE or iris to block the fluorescent signal. The time courses of calcium responses for four selected regions of interest (ROI)s surrounding GCaMP3 positive cells in the cornea near the scleral edge are shown (**A**). No light-evoked calcium elevations were observed in ROIs in cornea. (**B**, **C**) Shows full field pictures of fluorescent images at $t = 0$ and $t = 3$ s in the cornea. (**D**) Plots the time courses of 4 cells situated in the adjacent retina. These 4 randomly selected cells exhibited light-dependent calcium responses having times to peak around 3 s following light onset. (**E**, **F**) Shows full field pictures of fluorescent images at $t = 0$ and $t = 3$ s. (**G**) is a schematic drawing of a mouse eye showing how the eyes were cut in order to obtain tissue containing both the cornea and the retina. The vertical dotted line shows the cut line to remove a hemi dome-shaped section from the front of the cornea. The horizontal line shows one of the four radial cut lines that extended ~3/4 the distance from the limbic rim back toward the optic

nerve. (**H**) is a schematic drawing of the flattened corneal/retina tissue. No iris is shown because it was transparent in these albino mice.

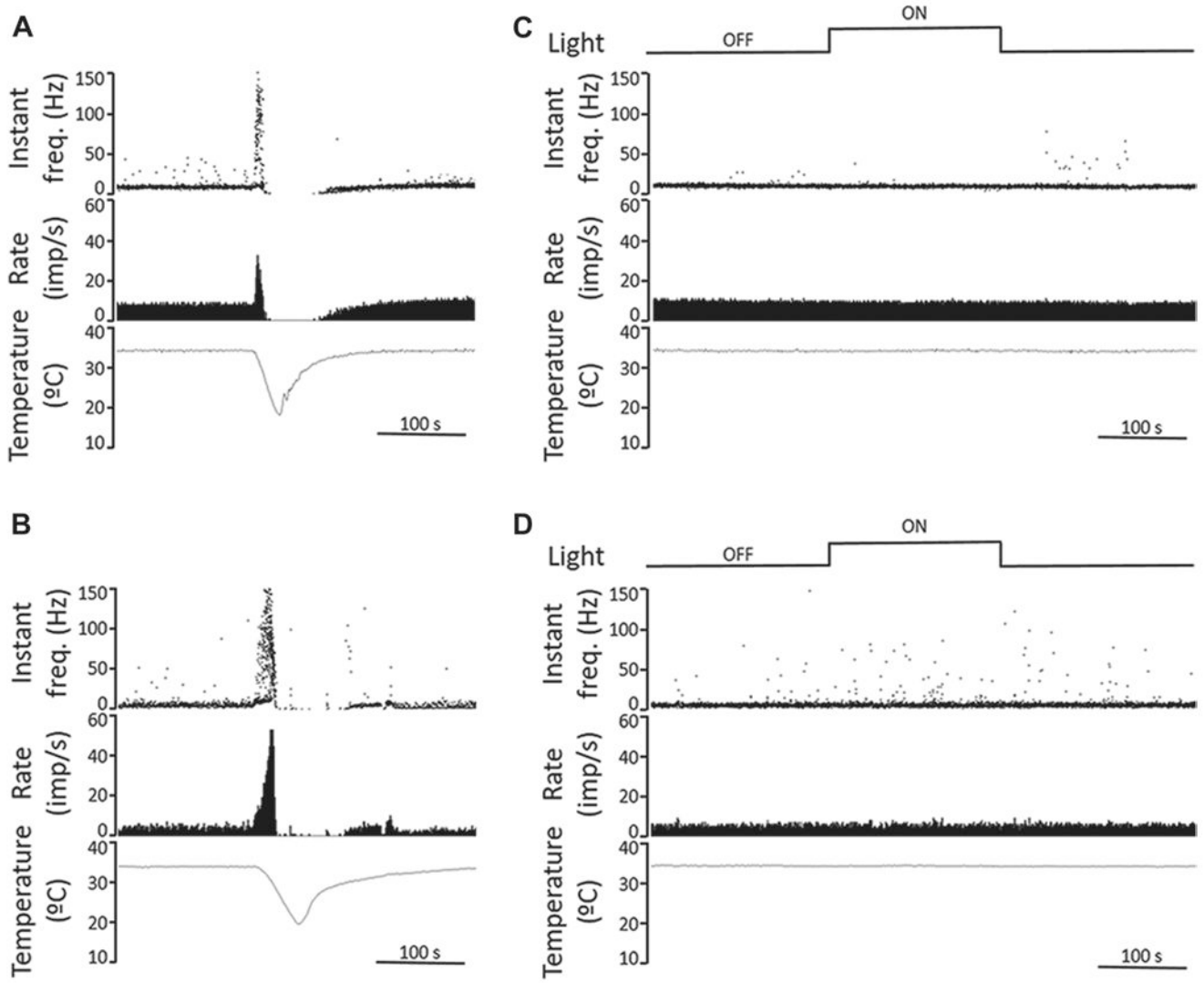

Fig. 5.

Recordings from corneal cold receptors in guinea pig and mouse corneas show no response to light. (**A**, **B**) Sample recordings of nerve terminal impulse (NTI) activity in response to a cooling ramp (from 34 to 20°C) of cold thermoreceptors recorded in a guinea pig (**A**) and a mouse cornea (**B**), performed in light condition. Once firing rate and temperature returned to baseline, the cornea was kept in darkness for 15 min. The upper traces plot the instantaneous frequency in Hz. The middle traces plot the time course of the NTI activity (in impulses/s). The lower traces display the temperature value measured at the perfusion chamber, near the corneal surface (in °C). (**C**, **D**) Effects of light on ongoing NTI activity at basal temperature (34°C) of cold thermoreceptors recorded in a guinea pig (**C**) and a mouse cornea (**D**). The second traces plot the instantaneous frequency in Hz, showing no differences in rhythmic firing pattern of the units under dark and light conditions (upper traces). The third and lower traces plot ongoing NTI activity (in impulses/s) at constant, basal temperature (lower traces). Time scales are 100 s.

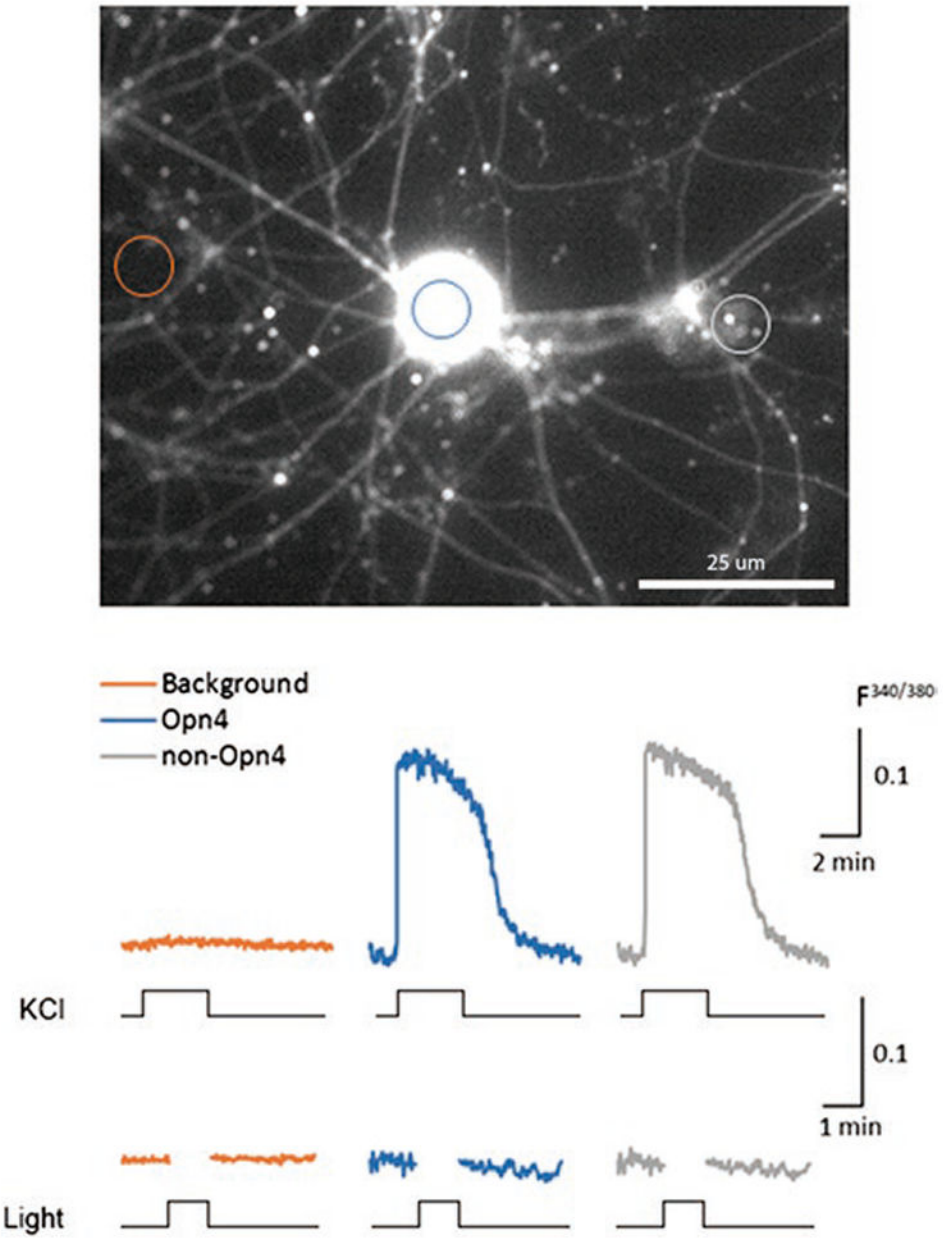

Fig. 6.

KCl but not light evokes responses in melanopsin-expressing TG neurons. Two-month-old cultured TG neurons harvested from *Opn4*^{cre}::Ai14 mice were transfected with AAV-hSvn-floxed EFGP virus (4 μl; 6 × 10^{12} titer). The premise of this method was that if cells were positive for EGFP, this increased the likelihood that melanopsin was being actively expressed. Two to three weeks after viral infection, cells on the coverslips were loaded with Fura-2 AM and 20% pluronic acid by incubating for 1 h at RT (see Materials and methods). Coverslips were individually placed in the perfusion chamber for imaging. Fluorescence in three types of ROIs was monitored. One class of ROIs was drawn on a nonfluorscent region of background. Other ROIs encircle Fura-2 loaded cells that did not show any EGFP signal.

The third type of ROI encircled those cells showing both EGFP and Fura-2 signal. We first compared responses to elevated potassium (50 mM). Both the Fura-2 loaded and EGFP plus Fura-2 loaded cells responded with a KCl-induced robust calcium elevation. We next stimulated the cells with light. No light responses were found. In our survey of three coverslips containing a total of more than 30 tdTomato and EGFP cells loaded with Fura-2 AM, we detected no light-induced calcium increases.